

# Cation Selectivity of and Cation Binding to the cGMP-dependent Channel in Bovine Rod Outer Segment Membranes

PAUL P. M. SCHNETKAMP

From the Department of Medical Biochemistry, University of Calgary, Calgary, Alberta T2N 4N1, Canada

**ABSTRACT** The properties of the cGMP-dependent channel present in membrane vesicles prepared from intact isolated bovine rod outer segments (ROS) were investigated with the optical probe neutral red. The binding of neutral red is sensitive to transport of cations across vesicular membranes by the effect of the translocated cations on the surface potential at the intravesicular membrane/water interface (Schnetkamp, P. P. M. *J. Membr. Biol.* 88: 249–262). Only 20–25% of ROS membrane vesicles exhibited cGMP-dependent cation fluxes. The cGMP-dependent channel in bovine ROS carried currents of alkali and earth alkali cations, but not of organic cations such as choline and tetramethylammonium; little discrimination among alkali cations ( $K > Na = Li > Cs$ ) or among earth alkali cations ( $Ca > Mn > Sr > Ba = Mg$ ) was observed. The cation dependence of cGMP-induced cation fluxes could be reasonably well described by a Michaelis-Menten equation with a dissociation constant for alkali cations of about 100 mM, and a dissociation constant for  $Ca^{2+}$  of 2 mM. cGMP-induced  $Na^+$  fluxes were blocked by  $Mg^{2+}$ , but not by  $Ca^{2+}$ , when the cations were applied to the cytoplasmic side of the channel. cGMP-dependent cation fluxes showed a sigmoidal dependence on the cGMP concentration with a Hill coefficient of 2.1 and a dissociation constant for cGMP of 92  $\mu M$ . cGMP-induced cation fluxes showed two pharmacologically distinct components; one component was blocked by both tetracaine and *L-cis* diltiazem, whereas the other component was only blocked by tetracaine.

## INTRODUCTION

Excised patches of plasma membrane of the outer segment of amphibian and mammalian rod photoreceptors (ROS) contain a cGMP-dependent conductance that in the intact cell appears to carry the light-sensitive current (Fesenko et al., 1985; Yau and Nakatani, 1985; Zimmerman et al., 1985; Matthews, 1987; Hanke et al., 1988; Quandt et al., 1988). cGMP-induced cation fluxes (mostly  $Ca^{2+}$ ) have also been described in preparations of both amphibian and bovine ROS membrane vesicles (Caretta et al., 1979, Caretta and Cavaggioni, 1983; Caretta, 1985; Koch and Kaupp, 1985; Schnetkamp and Bownds, 1987; Bauer, 1988). The cGMP-dependent channel has been purified and functionally reconstituted from bovine rods (Cook et al., 1987). The preparation of bovine ROS membrane vesicles offers an opportunity

to study the properties of the cGMP-dependent channel from mammalian ROS, a preparation less accessible to electrical recordings due to their small size. One point of distinction between the bovine and amphibian cGMP-dependent channels has been reported: cGMP-dependent  $\text{Ca}^{2+}$  fluxes in bovine ROS show two pharmacologically distinct components (Koch et al., 1987; Schnetkamp, 1987), while only a single component is observed in frog ROS (Nicol et al., 1987). In this study I have used a recently developed optical technique to measure electrogenic cation fluxes in a suspension of membrane vesicles (Schnetkamp, 1985*a, b*). The cation selectivity of and cation binding to the cGMP-dependent channel in bovine ROS membranes were measured, and the results are compared with those obtained for the light-sensitive and cGMP-dependent conductance observed in the amphibian rod. In addition, the cGMP-dependent channel offers a case to illustrate an optical probe for measuring small ionic currents not in single cells, but in a suspension of cells or cellular organelles.

#### MATERIALS AND METHODS

##### *Preparation of ROS Membrane Vesicles*

Bovine eyeballs were purchased from a local abattoir and collected as fresh as possible in a light-tight container. ROS with a sealed plasma membrane were isolated and purified as  $\text{Ca}^{2+}$ -rich or  $\text{Ca}^{2+}$ -depleted intact ROS as described before (Schnetkamp, 1986). In the  $\text{Ca}^{2+}$ -depleted preparation dithiothreitol (0.5 mM) was present throughout the procedure. After purification and washing, intact ROS were resuspended to a final concentration of 150–250  $\mu\text{M}$  rhodopsin in a medium containing 600 mM sucrose, 5% wt/vol Ficoll 400, 0.5 mM dithiothreitol, and 20 mM HEPES (adjusted to pH 7.4 with arginine). The suspension was immediately frozen by putting its container in an ethanol/dry ice bath. After thawing, the ROS suspension was subjected to a hypotonic shock by a 20-fold dilution in 10 mM HEPES (adjusted to pH 7.4 with arginine); after 2 min, 25 mM tetramethylammonium chloride (TMACl) was added from a 2.5 M stock solution to facilitate sedimentation of ROS membranes by centrifugation (20 min at 10,000 rpm or 12,000 *g* in a J-20 rotor [Beckman Instruments, Inc., Palo Alto, CA]). The supernatant was discarded and the pellet resuspended to a final rhodopsin concentration of 200–300  $\mu\text{M}$  in a medium containing 300 mM sucrose, 2.5% Ficoll 400, 0.5 mM dithiothreitol, and 20 mM HEPES (adjusted to pH 7.4 with arginine); this preparation will be referred to as ROS membrane vesicles. Measurements of cGMP-induced cation fluxes were completed within 60 min. All the above and the following procedures were carried out under dim red light illumination.

After the above protocol cGMP-independent cation fluxes in ROS membrane vesicles were minimized, and no such permeabilities appeared to be present in membranes derived from  $\text{Ca}^{2+}$ -depleted ROS. In membranes derived from  $\text{Ca}^{2+}$ -rich ROS that were not immediately frozen, a significant  $\text{K}^+$  permeability was frequently observed in the absence of cGMP. No experiments on the cGMP-independent  $\text{K}^+$  permeability are reported here.

##### *Measurement of Cation Fluxes across ROS Membrane Vesicles*

Cation fluxes across ROS membrane vesicles were measured with the optical probe neutral red as described before (Schnetkamp et al., 1981; Schnetkamp, 1985*a, b*; Schnetkamp and Szerencsei, 1989). The physicochemical basis of this method is illustrated schematically in Fig. 1. Neutral red adsorbs to phospholipid bilayer membranes carrying a net negative charge (for example due to the presence of acidic phospholipids such as phosphatidylserine and

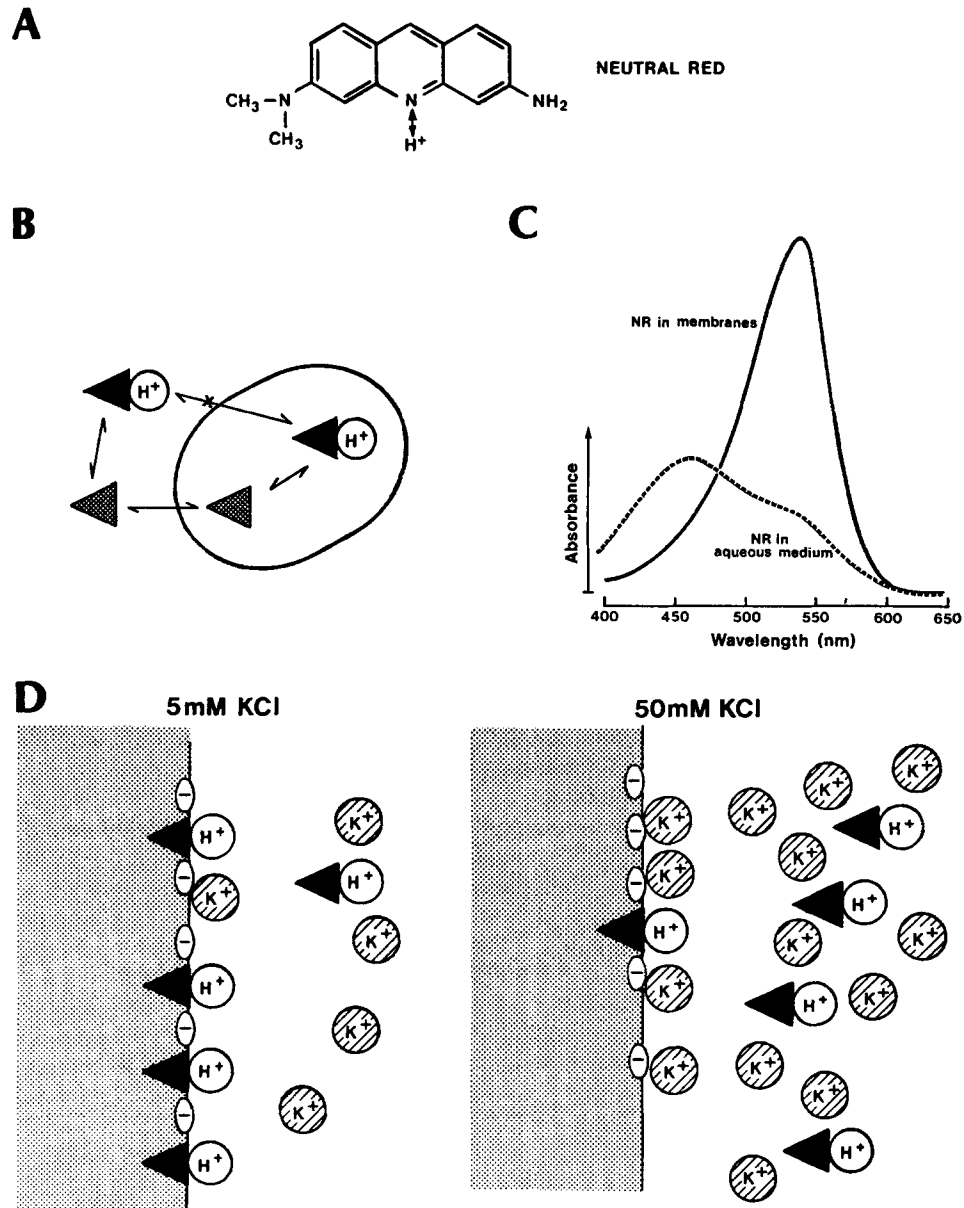


FIGURE 1. Neutral red as a probe for surface potentials. *A*, Molecular structure of neutral red; the arrow indicates the site of protonation. *B*, Neutral red readily crosses biological membranes in the uncharged basic form, but not in the positively charged acidic form. *C*, Absorption spectrum of equal concentrations of neutral red at pH 7.4 in aqueous solution (broken line) or adsorbed to ROS membranes (solid line). *D*, Effect of cation concentration on amount of neutral red adsorbed to membrane surface.

phosphatidylinositol); at pH 7.4 the neutral red adsorbed to the membrane is fully protonated, whereas neutral red in aqueous solution is predominantly unprotonated (Schnetkamp et al., 1981). As a consequence, membrane-bound neutral red can be distinguished easily from its aqueous counterpart in a spectrophotometer. In a dual wavelength spectrophotometer, a change in the difference in absorption  $A_{540} - A_{650}$  is a quantitative measure for a change in the amount of membrane-bound dye. Two forces control the binding of a positively charged amphiphile such as neutral red to phospholipid bilayers: first, the electrostatic surface potential as illustrated in Fig. 1; second, the transmembrane potential in the case that the charged form of neutral red can cross the bilayer membrane. The binding of neutral red to ROS membranes is not affected by changes in membrane potential (Schnetkamp and Szerencsei, 1989), leaving the electrostatic surface potential as the dominant parameter controlling changes in binding of neutral red to ROS membranes. Thus, the binding of the positively charged protonated form of neutral red is a function of the electrostatic surface potential at the membrane/water interface, which in turn is a simple function of the concentration and valency of the cations in the aqueous solution (as illustrated in Fig. 1 by potassium ions). In the next section I will demonstrate that changes in the binding of neutral red to the intravesicular membrane surface (measured by the change in the difference of absorption  $A_{540} - A_{650}$ ) can provide a quantitative measure for cation fluxes across the vesicle membrane (see Fig. 2).

The suspension of ROS membranes was diluted to final concentration of 20  $\mu\text{M}$  rhodopsin in 300 mM sucrose, 0.5 mM dithiothreitol, 50  $\mu\text{M}$  neutral red, 20 mM HEPES (adjusted to pH 7.4 with arginine), and 1  $\mu\text{M}$  FCCP when indicated. Aliquots of 2 ml were placed in a cuvette, kept at a constant temperature by means of a circulating waterbath, and mixed with a magnetic spinbar. The difference in light absorption ( $A_{540} - A_{650}$ ) upon addition of the various cations, cGMP, and ionophores was monitored in a DW2C dual wavelength spectrophotometer (SLM-Aminco, Urbana, IL).

Four control experiments were done to ensure that the cGMP-induced changes in light absorption in the presence of alkali cations were due to changes in the binding of neutral red, and not to other causes. First, when the compartment containing the cGMP-dependent channel was equilibrated with alkali cations by a first addition of either cGMP (500  $\mu\text{M}$ ) or gramicidin, a second addition of cGMP (500  $\mu\text{M}$ ) did not elicit any absorption change other than that due to dilution (0.002 absorbance units). Second, addition of cGMP in the absence of the dye neutral red did not elicit any absorption change. Third, addition of cGMP in the presence of impermeable cations such as choline and tetramethylammonium did not elicit any absorption change. Finally, cGMP-induced changes in the binding of neutral red were not due to an acidification of the medium caused by hydrolysis of cGMP; no hydrolysis of cGMP occurred as tested with the pH-indicating dye phenol red (activation of the rod phosphodiesterase required the presence of GTP). In all experiments cGMP was added from concentrated stock solutions in a volume of 5  $\mu\text{l}$  to a total volume in the cuvette of 2 ml. The starting value for  $A_{540} - A_{650}$  amounted to  $\sim 1.5$ .

#### *Calibration of cGMP-induced Cation Fluxes*

In all experiments reported in this study, cGMP-induced cation influx into ROS membrane vesicles was electrically compensated for by an efflux of protons via the electrogenic protonophore FCCP. Therefore, it is possible to obtain a quantitative calibration of cation flux as indicated by the cGMP- or gramicidin-induced changes in light absorption due to the unbinding of neutral red by measuring the proton efflux with the pH-indicating dye phenol red. Phenol red does not bind to ROS membranes and reports on the pH in the suspension medium (Schnetkamp and Kaupp, 1985); under our experimental conditions pH-indicating absorption changes were linearly related to the amount of HCl added. In this experiment,

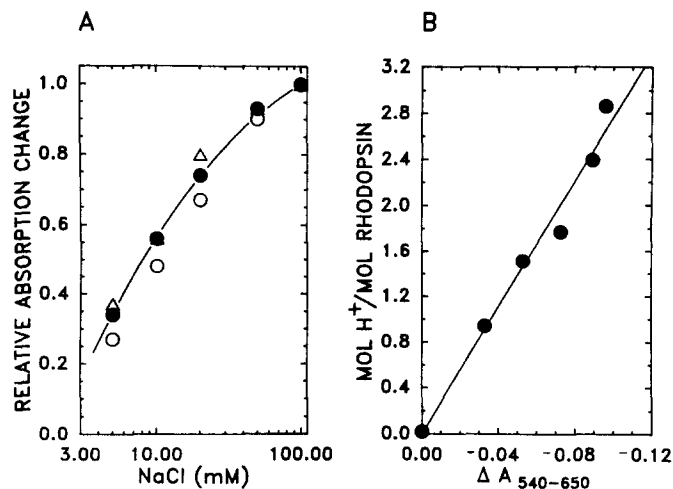


FIGURE 2. Calibration of cation flux across ROS membrane vesicles as a function of cation-induced changes in light absorption due to unbinding of neutral red at the intravesicular membrane/water interface. *A*, Na<sup>+</sup>-induced release of neutral red from the intravesicular surface (solid circles) was compared with (a) Na<sup>+</sup>-induced release of neutral red from the extravesicular surface (open circles) and (b) Na<sup>+</sup>-induced proton release from the intravesicular surface (triangles). The suspension medium of ROS membrane vesicles in the neutral red experiments contained 300 mM sucrose, 50  $\mu$ M neutral red, and 20 mM HEPES (brought to pH 7.4 with arginine); the suspension medium of ROS membrane vesicles in the proton release measurements contained 300 mM sucrose, 20 mM tetramethylammonium chloride, 40  $\mu$ M phenol red, and 0.5 mM HEPES (brought to pH 7.4 with arginine). All measurements were done in the dual wavelength mode as  $A_{540} - A_{650}$  (neutral red) or  $A_{570} - A_{650}$  (phenol red). Absorption changes were normalized by dividing the value observed at each given Na<sup>+</sup> concentration by the value observed for the highest Na<sup>+</sup> concentration of 100 mM. Neutral red release from the extravesicular membrane surface was measured by the instantaneous absorption changes upon addition of NaCl; release of neutral red from the intravesicular surface was measured by the absorption changes in the presence of extravesicular Na<sup>+</sup> observed upon addition of gramicidin. Absorption changes originating from the intravesicular membrane surface were typically twice as large as those originating from the extravesicular membrane surface. Proton release from the intravesicular space was measured by the ( $A_{570} - A_{650}$ ) upon addition of gramicidin 10 s after addition of NaCl. *B*, Na<sup>+</sup>-induced proton release from the intravesicular space (measured with the pH-indicating dye phenol red) was compared with Na<sup>+</sup>-induced changes in the binding of neutral red to the intravesicular membrane surface (measured as  $A_{540} - A_{650}$ ). Absorption changes by the dye phenol red were calibrated into moles H<sup>+</sup> release/mole rhodopsin by adding known amounts of HCl to the suspension.

ROS membrane vesicles were made permeable to Na<sup>+</sup> and protons by addition of the channel ionophore gramicidin. Fig. 2 *A* compares the dependence on Na<sup>+</sup> concentration of (a) the amplitude of Na<sup>+</sup>-induced unbinding of neutral red from the extradiskal membrane surface, (b) the amplitude of the Na<sup>+</sup>-induced unbinding of neutral red from the intradiskal membrane surface, and (c) the Na<sup>+</sup>-induced release of protons from the intradiskal space; the amplitudes of all three parameters depended on the external Na<sup>+</sup> concentration in a very similar manner. The relatively large changes observed between 1 and 10 mM are typical for Na<sup>+</sup>-induced

screening of surface potentials (Schnetkamp, 1985a).  $\text{Na}^+$ -induced changes in light absorption due to unbinding of neutral red were linearly related to  $\text{Na}^+$ -induced proton release (Fig. 2 B) and can be converted in a quantitative measurement of  $\text{Na}^+$  flux. The above results could be interpreted to indicate that neutral red bound to the surface of ROS membranes acts as a pH indicator at the membrane surface rather than as an indicator of surface potential; these two mechanisms are indistinguishable since the surface potential controls the surface pH, and hence the degree of protonation of acidic and basic groups on the membrane surface. Sodium ions (or any other cation) entering the intravesicular space replace protons as counterions for the fixed negatively charged groups on the membrane. Neutral red and protons both carry a single positive charge and their binding to the membrane depends in an identical way on the surface potential and cation-induced changes thereof. The observation that changes in neutral red binding on the external and internal membrane surface, respectively, and proton release from the intravesicular space were all very similar with respect to their dependence on the  $\text{Na}^+$  concentration, supports the conclusion that  $\text{Na}^+$ -induced proton release is mediated by  $\text{Na}^+$ -induced changes in surface potential and a concomitant degree of protonation of membrane components. The issue of intravesicular pH changes is discussed in more detail in Schnetkamp (1985a).

## RESULTS

### *cGMP-induced $\text{Na}^+$ Transport in Membrane Vesicles Derived from Intact Bovine ROS*

In the first experiment I describe the basic observation on cGMP-induced changes in  $\text{Na}^+$  flux in membrane vesicles derived from intact ROS after freeze-thawing and hypotonic shock; this preparation consists of pieces or vesicles of inverted plasma membrane with the disks attached to them via filamentary structures (Molday et al., 1987). Closed vesicles could be vesicles of inverted plasma membrane, intact disks, or perhaps vesicles of fused disk and plasma membrane. In the following sections I will use the term ROS membrane vesicles to indicate the ensemble of closed membrane vesicles derived from intact bovine ROS. In order to be detected with the method used in this study, cGMP-dependent channels have to reside in sealed vesicles with the cGMP binding sites of the channel on the extravesicular membrane surface.

Addition of 100 mM NaCl to a suspension of ROS membrane vesicles in a buffered sucrose medium containing 50  $\mu\text{M}$  neutral red and 1  $\mu\text{M}$  FCCP caused an instantaneous change in absorption ( $A_{540} - A_{650}$ ) due to dilution and to  $\text{Na}^+$ -induced unbinding of neutral red from the external surface of the membrane vesicles (Fig. 2). The instantaneous change in light absorption was followed by time-resolved changes indicating unbinding of neutral red from the intravesicular membrane surface; a typical example is depicted in Fig. 3. As discussed in the Methods, the unbinding of neutral red is most likely caused by  $\text{Na}^+$ -induced changes in the surface potential at the intravesicular membrane/water interface and therefore reflects  $\text{Na}^+$  transport into the vesicles. Addition of the ionophore gramicidin, a nonselective channel for alkali cations, caused a rapid unbinding of neutral red from the intravesicular membrane surface, consistent with a rapid increase in the intravesicular  $\text{Na}^+$  concentration due to  $\text{Na}^+$  influx via gramicidin. The calibration plot illustrated in Fig. 2 can be used to convert changes in light absorption due to

unbinding of neutral red into quantitative cation fluxes independent of the molecular mechanism underlying the unbinding of neutral red.

In the absence of gramicidin or cGMP,  $\text{Na}^+$  influx into ROS membrane vesicles ranged from 0 to 0.1 pA when expressed as a current through the ensemble of vesicles derived from a single bovine ROS. In this and subsequent calculations I assumed that the total rhodopsin concentration in bovine ROS amounts to 3 mM and that a single bovine ROS is a cylinder of  $1 \times 20 \mu\text{m}$  and contains  $2.9 \times 10^7$  rhodopsin molecules.

Addition of 500  $\mu\text{M}$  cGMP before addition of gramicidin caused a rapid increase in the rate of absorption change in the same direction as that observed for gramicidin. However, the amplitude of the cGMP-induced absorption change amounted to only 20% of that observed for gramicidin; a value of 20–25% was

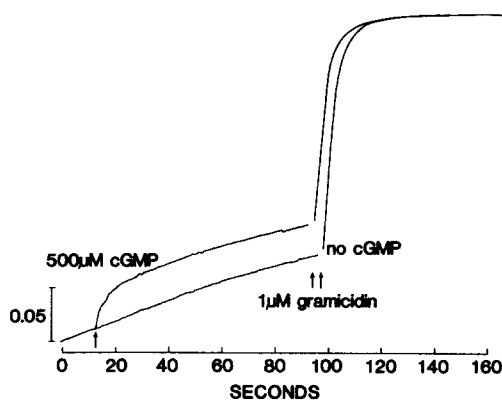


FIGURE 3. cGMP- and gramicidin-induced  $\text{Na}^+$  fluxes across ROS membrane vesicles. ROS membrane vesicles were suspended in 300 mM sucrose, 50  $\mu\text{M}$  neutral red, 1  $\mu\text{M}$  FCCP, and 20 mM HEPES (adjusted to pH 7.4 with arginine), final rhodopsin concentration 20  $\mu\text{M}$ . Records illustrated were obtained in the dual wavelength mode:  $-(A_{540} - A_{650})$ ; an upward deflection indicates an increase in intravesicular cation concentration. To the above suspension 100 mM NaCl was added

10 s before the start of the recordings; at the first arrow 500  $\mu\text{M}$  cGMP was added to the recording so labeled. At the second and third arrows, 90–95 s after the start of the traces 1  $\mu\text{M}$  gramicidin was added in both recordings. The calibration bar represents 0.05 absorbance units. Temperature, 25°C. The recordings shown in this and all subsequent figures were traced by hand from the original recordings. The noise in the recordings did not reflect photometric sensitivity, but was caused by the spin bar used to mix the suspension.

observed consistently in many preparations of ROS membrane vesicles. This result suggests that cGMP opens an  $\text{Na}^+$ -permeable channel. Adding gramicidin after addition of cGMP caused a rapid change in light absorption to the same value as that observed when only gramicidin was added, whereas addition of cGMP after addition of gramicidin did not cause any absorption change (not shown). The effects of gramicidin and cGMP were not additive, i.e., membrane vesicles equilibrated with  $\text{Na}^+$  via the cGMP-dependent channel did not take up any further  $\text{Na}^+$  after addition of gramicidin. The average cGMP-induced  $\text{Na}^+$  flux in ROS membrane vesicles (derived from a single ROS) at 100 mM  $\text{Na}^+$  amounted to  $5 \times 10^6$   $\text{Na}^+$ /outer segment per s or a current of 0.8 pA; flux rates were obtained by measuring the initial rate of cGMP-induced change in light absorption and converting this into flux with the calibration curve shown in Fig. 2.

*cGMP-induced Na<sup>+</sup> Fluxes Reflect a Conductance Mechanism*

In the above experiment I used the electrogenic protonophore FCCP with the objective of providing an outward proton current to compensate for the putative cGMP-induced inward Na<sup>+</sup> current; this aspect is investigated in more detail in the experiments illustrated in Fig. 4 A. Addition of cGMP in the presence of an inward gradient of Na<sup>+</sup> did not cause a rapid change in light absorption in the absence of FCCP. For comparison, traces are included for the absorption changes when no cGMP was added, or when Na<sup>+</sup> was replaced with the impermeable cation tetra-

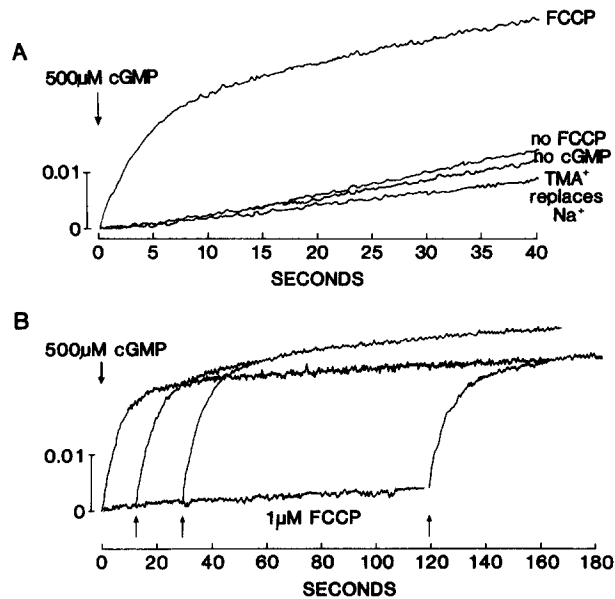


FIGURE 4. cGMP-induced Na<sup>+</sup> fluxes reflect cGMP-induced Na<sup>+</sup> currents. Experimental conditions were as described in the legend of Fig. 3; 100 mM NaCl was added 10 s before the start of the recordings and 500 μM cGMP was added at time zero. The calibration bar represents a change in light absorption by 0.01 absorbance unit. Temperature, 25°C. A, Recordings are labeled to indicate the omission of FCCP (no FCCP), omission of cGMP (no cGMP), replacement of Na<sup>+</sup> by tetramethylammonium ion (TMA<sup>+</sup>), and control (FCCP). B, The recordings were started by addition of 500 μM cGMP 10 s after addition of 100 mM NaCl. The arrows indicate the time of addition of FCCP. In the recording that showed an immediate response to addition of cGMP, FCCP was present at the start.

methylammonium. In a parallel experiment I measured cGMP-induced proton release from ROS membrane vesicles with the pH-indicating dye phenol red (with a protocol similar to that used for the experiment illustrated in Fig. 2); addition of cGMP in the presence of an inward gradient of Na<sup>+</sup> caused very little proton release unless FCCP was present (not illustrated). A likely explanation for the above observations is that in the absence of FCCP little mass influx of Na<sup>+</sup> via the cGMP-dependent channel occurred, but instead an inside-positive membrane potential developed. In the presence of FCCP, the cGMP-induced influx of Na<sup>+</sup> appeared



to be compensated for by an efflux of protons. FCCP does not appear to have a pharmacological effect on the cGMP-dependent channel as judged from the observation that FCCP had no effect on cGMP-induced  $\text{Ca}^{2+}$  release measured with arsenazo III (not illustrated). cGMP-induced  $\text{Ca}^{2+}$  release was observed in the absence of any ionophores (Caretta and Cavaggioni, 1983; Koch and Kaupp, 1985; Schnetkamp, 1987; Bauer, 1988). In the above studies cGMP-induced  $\text{Ca}^{2+}$  release was probably electrically compensated for by cGMP-induced alkali cation influx and no net current presumably occurred (discussed in Koch and Kaupp, 1985; Schnetkamp, 1987).

#### *Do cGMP-induced $\text{Na}^+$ Fluxes Inactivate?*

The amplitude of the cGMP-induced changes in light absorption was much smaller compared with that induced by gramicidin (Fig. 3). This could be interpreted in two ways: it could reflect inactivation of the cGMP-dependent channels a few seconds after opening, or it could suggest that only 20% of the membrane vesicles contained a functional cGMP-dependent channel. The use of FCCP offers an opportunity to investigate the possibility of inactivation of the cGMP-dependent channel. In this experiment cGMP was added to ROS membrane vesicles immediately after establishment of an inward  $\text{Na}^+$  gradient, but before addition of FCCP; after some time interval FCCP was added to initiate a net inward  $\text{Na}^+$  flux and outward proton flux. Increasing the time interval between additions of cGMP and FCCP, respectively, should give rise to progressively smaller signals if the cGMP-dependent channels inactivate in this time interval (Fig. 4 B). This is not observed, demonstrating that the cGMP-dependent channel does not inactivate on a time scale of 2 min.

#### *Cation Selectivity of the cGMP-dependent Channel*

The cation selectivity of the cGMP-dependent channel was investigated in the experiments illustrated in Fig. 5 and summarized in Table I. Most of the experiments with alkali cations were conducted at a temperature of 5°C, which decreased the rate of cGMP-induced cation fluxes by about fivefold compared with those observed at 25°C (Fig. 5; note that the traces are separated by 0.01 absorption units). The first thing that can be noticed in Fig. 5 is that the amplitude of the cGMP-induced absorption changes was identical for the different alkali cations tested; this is consistent with the notion that electrostatic screening of surface potentials by cations is independent of the type of cation; it suggests that screening rather than charge compensation (binding) is the dominant mechanism by which alkali cations reduce the surface potential. The amplitude of the cGMP-induced signals observed for divalent cations (tested at 20 mM) was somewhat more variable, suggesting that charge compensation (binding) contributes to the reduction of surface potential by divalent cations (not illustrated); this result can be anticipated from similar effects of divalent cations on the surface potential of simple phospholipid bilayer membranes (McLaughlin et al., 1978, 1981). The ion selectivity of cation fluxes through the cGMP-dependent channel was obtained by measuring the initial rates of cGMP-induced light absorption changes in the presence of different cations; the measurements are equivalent to electrically recorded conductance ratios and the results are

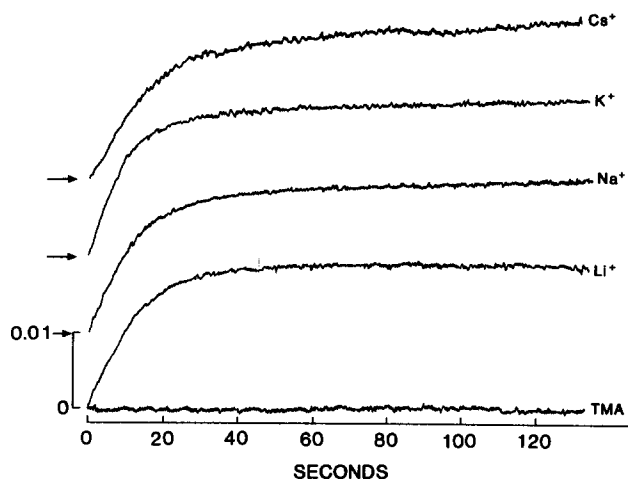


FIGURE 5. Ion selectivity of cGMP-induced alkali cation fluxes. Experimental conditions were as in the legend of Fig. 3; 100 mM of the indicated cation chlorides was added 10 s before addition of 500  $\mu$ M cGMP at time zero. TMA is tetramethylammonium ion. Note that the recordings are separated by 0.01 absorbance units. Temperature, 5°C.

summarized in Table I. No cGMP-induced fluxes were observed for the organic cations tetramethylammonium and choline.

The cGMP-induced  $\text{Ca}^{2+}$  currents (at 20 mM  $\text{Ca}^{2+}$ ) were on average 3.5-fold smaller (SD = 0.9, 13 preparations) as compared with cGMP-induced  $\text{Na}^+$  currents (at 100 mM  $\text{Na}^+$ ); i.e., the cGMP-induced  $\text{Ca}^{2+}$  flux was 7-fold smaller than the cGMP-induced  $\text{Na}^+$  flux.

TABLE I  
*Cation Selectivity of the cGMP-dependent Channel in Bovine ROS*

Cation	Relative fluxes	Standard deviation	No. of observations
$\text{Li}^+$	0.83	0.12	8
$\text{Na}^+$	0.88	0.10	8
$\text{K}^+$	=1.00		
$\text{Cs}^+$	0.59	0.10	7
$\text{Mg}^{2+}$	0.50	0.10	11
$\text{Mn}^{2+}$	0.86	0.26	5
$\text{Ca}^{2+}$	=1.00		
$\text{Sr}^{2+}$	0.64	0.09	10
$\text{Ba}^{2+}$	0.47	0.07	10

cGMP-induced alkali cation fluxes were measured at 500  $\mu$ M cGMP and 100 mM of the cation chloride salts; fluxes were normalized with respect to the fluxes of the most conductive cation  $\text{K}^+$ . cGMP-induced divalent cation fluxes were measured at 500  $\mu$ M cGMP and 20 mM of the divalent cation chloride salts; fluxes were normalized with respect to the fluxes of the most conductive divalent cation  $\text{Ca}^{2+}$ . Results from experiments conducted at 5 and 25°C were pooled; no difference in ion selectivity was apparent when experiments conducted at 5°C were compared with those conducted at 25°C.

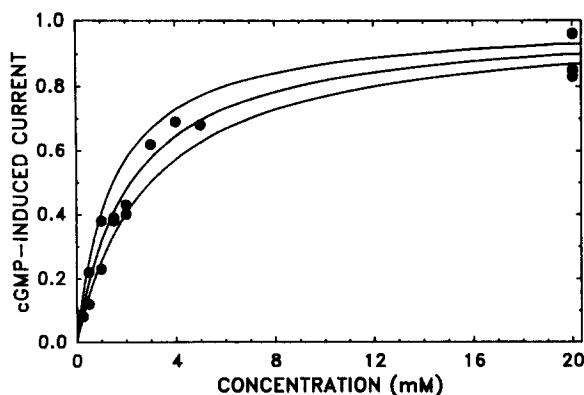


FIGURE 6.  $\text{Ca}^{2+}$ -dependence of cGMP-induced  $\text{Ca}^{2+}$  fluxes. cGMP-induced  $\text{Ca}^{2+}$  fluxes were measured as a function of  $\text{Ca}^{2+}$  concentration following the protocol described in Figs. 3 and 5. The flux rate or current was normalized with respect to the maximal current extrapolated from the data; maximal current and dissociation constant were obtained from a linear regression of a Scatchard plot of the data. The disso-

sociation constant obtained was 2.2 mM. The computer-drawn curves represent Michaelis-Menten equations with, from top to bottom,  $\text{Ca}^{2+}$  dissociation constants of 1.5, 2.2, and 3.0 mM. Temperature, 25°C.

#### *Cation Binding to the cGMP-dependent Channel*

The cGMP-induced cation fluxes were dependent on the external cation concentration; both for  $\text{Ca}^{2+}$  and alkali cations the dependence of cGMP-induced flux rate on the external cation concentration was reasonably well described by a single-site Michaelis-Menten equation (Figs. 6 and 7). This suggests that the cGMP-dependent channel has a binding site for  $\text{Ca}^{2+}$  with a dissociation constant of 2 mM (Fig. 6), and a binding site for alkali cations with dissociation constants between 75 and 150 mM (Fig. 7).

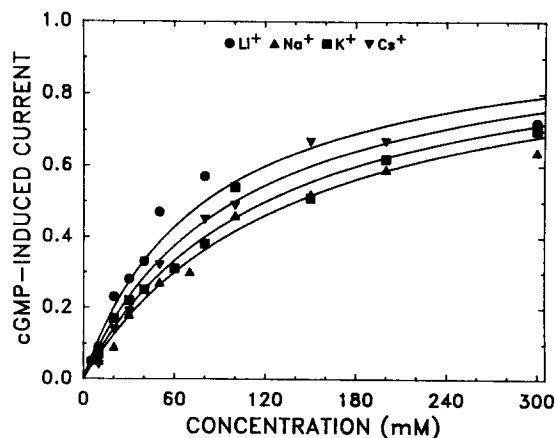


FIGURE 7. Alkali cation dependence of cGMP-induced alkali cation fluxes. cGMP-induced alkali cation fluxes were measured as a function of cation concentration following the protocol described in Figs. 3 and 5. The flux rate or current was normalized with respect to the maximal current extrapolated from the data; maximal current and dissociation constant were obtained separately for each cation from a linear regression of a Scatch-

ard plot of the data. The dissociation constants obtained were 80 mM ( $\text{Li}^+$ , circles), 144 mM ( $\text{Na}^+$ , triangles), 120 mM ( $\text{K}^+$ , squares), and 101 mM ( $\text{Cs}^+$ , inverted triangles). The computer-drawn curves represent Michaelis-Menten equations with, from top to bottom, dissociation constants of 80, 100, 120, and 140 mM. Temperature, 5°C.

*Interaction between Cations in the cGMP-dependent Channel*

The experiments illustrated in Figs. 6 and 7 show that the cGMP-dependent channel has a higher affinity for  $\text{Ca}^{2+}$  as compared with  $\text{Na}^+$  or other alkali cations; consistent with this, cGMP-induced  $\text{Ca}^{2+}$  fluxes at saturating  $\text{Ca}^{2+}$  concentration were smaller than cGMP-induced  $\text{Na}^+$  fluxes at saturating  $\text{Na}^+$  concentration, since  $\text{Ca}^{2+}$  probably resided longer in the channel than  $\text{Na}^+$ . Therefore, the combined cGMP-induced cation flux in the presence of both  $\text{Ca}^{2+}$  and  $\text{Na}^+$  is expected to be

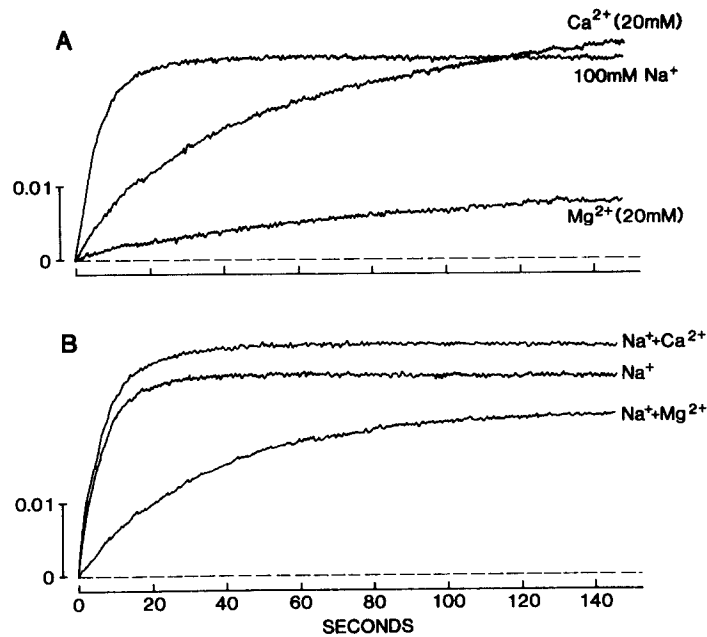


FIGURE 8. Effect of  $\text{Ca}^{2+}$  and  $\text{Mg}^{2+}$  on cGMP-induced  $\text{Na}^+$  fluxes. Experimental conditions were as described in the legend of Fig. 3. *A*, Cation concentrations were as indicated. *B*,  $\text{Na}^+$  concentration was 100 mM,  $\text{Ca}^{2+}$  and  $\text{Mg}^{2+}$  concentrations were 20 mM. Cations were added 10 s before addition of 500  $\mu\text{M}$  cGMP at time zero. The broken line represents fluxes in the absence of cGMP; in the vesicle preparation used for this experiment no cation leak fluxes were observed in the absence of cGMP. Temperature, 5°C.

less than the cGMP-induced cation flux in the presence of  $\text{Na}^+$  alone; i.e.,  $\text{Ca}^{2+}$  is expected to block  $\text{Na}^+$  fluxes. The experiment illustrated in Fig. 8 shows that this is not the case. cGMP-induced fluxes for the individual ionic species  $\text{Na}^+$ ,  $\text{Ca}^{2+}$ , and  $\text{Mg}^{2+}$ , respectively, are shown in Fig. 8 *A*; when applied to the cytoplasmic side of the channel  $\text{Mg}^{2+}$ , but not  $\text{Ca}^{2+}$ , inhibited cGMP-induced  $\text{Na}^+$  fluxes (Fig. 8 *B*) in agreement with observations on the cGMP-dependent channel in toad rods (Yau et al., 1986). The cGMP-induced  $\text{Na}^+$  and  $\text{Ca}^{2+}$  fluxes were additive at concentrations below their respective dissociation constants (not illustrated).

*Dependence of cGMP-dependent Fluxes on cGMP Concentration*

The cGMP-induced, cation-selective fluxes illustrated so far were all recorded at a saturating concentration of 500  $\mu\text{M}$  cGMP. Fig. 9 A illustrates the dependence of  $\text{Na}^+$  fluxes on the concentration of cGMP. The cGMP-induced  $\text{Na}^+$  flux depended

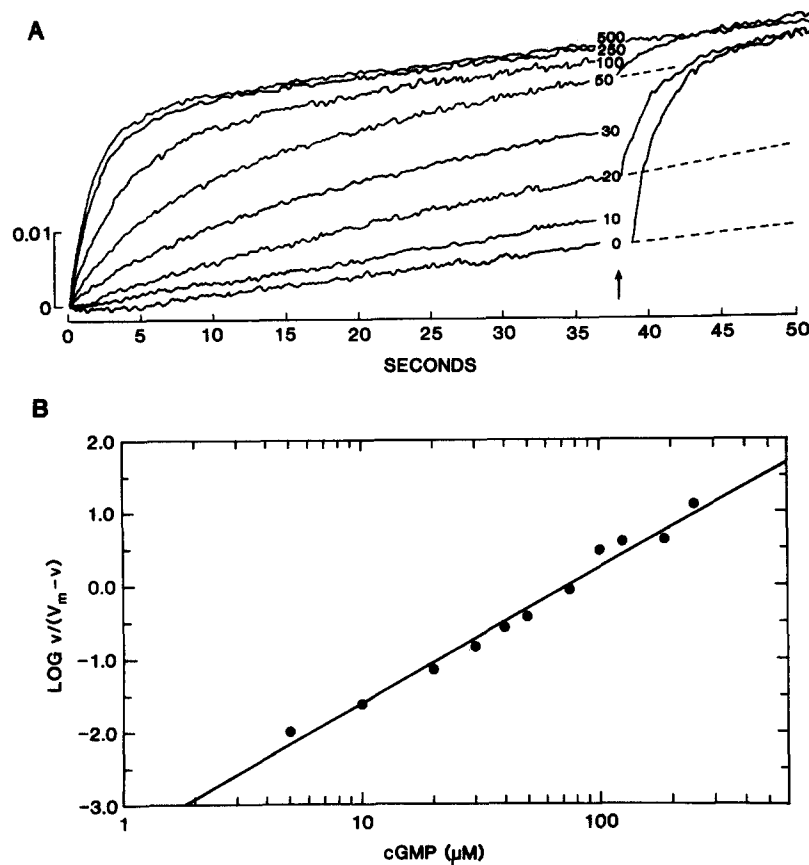


FIGURE 9. cGMP-induced  $\text{Na}^+$  fluxes as a function of cGMP concentration. A, Experimental conditions were as described in the legend of Fig. 3. 100 mM NaCl was added 10 s before addition of cGMP to the indicated final concentrations (micromolar) at time zero. The arrow (at  $\sim 38$  s) indicates addition of 500  $\mu\text{M}$  cGMP to the recordings to which previously were added 0, 20, and 50  $\mu\text{M}$  cGMP, respectively. Temperature, 25°C. B, Hill plot of cGMP dependence of cGMP-induced  $\text{Na}^+$  fluxes. The initial rates ( $v$ ) of cGMP-induced  $\text{Na}^+$  fluxes as a function of cGMP concentration were transformed into a Hill plot;  $V_m$  represents the maximal current at high cGMP concentration.

in a sigmoidal manner on the cGMP concentration; the data were transformed into a Hill plot which yielded a straight line with a Hill coefficient of 2.0 and a dissociation constant for cGMP of 75  $\mu\text{M}$  (Fig. 9 B). The cGMP-induced fluxes of the different alkali cations tested did not differ significantly in their dependence on the concen-

tration of cGMP; in six different preparations the average dissociation constant for cGMP was  $92 \mu\text{M}$  (SD = 9) and the average Hill coefficient was 2.12 (SD = 0.11).

*Evidence for the Existence of Two Distinct Forms of the cGMP-dependent Channel*

Previous studies with bovine ROS membrane vesicles showed that the cGMP-induced  $\text{Ca}^{2+}$  flux measured with arsenazo III had two components with different kinetics, with different dependence on cGMP concentration, and with a different pharmacology; similar experiments in frog ROS revealed only a single component (Koch et al.,

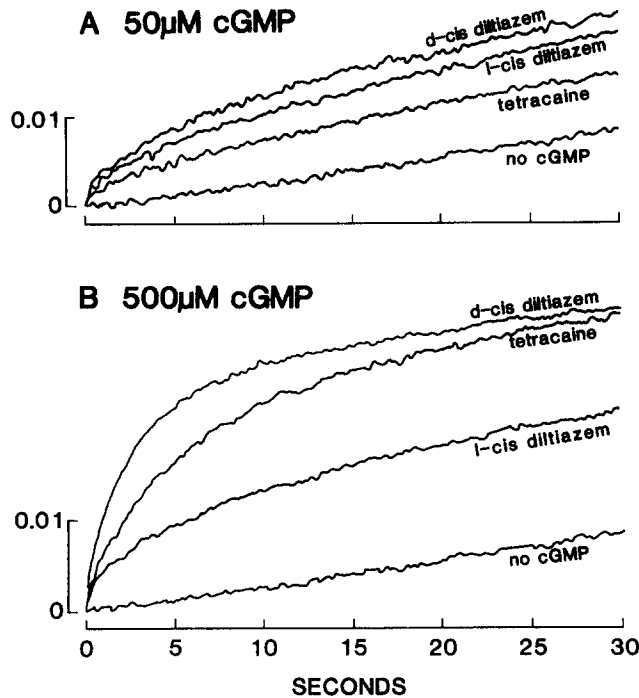


FIGURE 10. Pharmacology of cGMP-induced fluxes. Experimental conditions were as described in the legend of Fig. 3. 100 mM NaCl was added 10 s before addition at time zero of  $50 \mu\text{M}$  cGMP (A) or  $500 \mu\text{M}$  cGMP (B). No cGMP was added in the recordings labeled "no cGMP." Tetracaine and the two stereoisomers of diltiazem were present at a final concentration of  $20 \mu\text{M}$  as indicated; D-*cis* diltiazem reduced the amplitude of cGMP-induced changes in light absorption by 25%. Temperature,  $25^\circ\text{C}$ .

1987; Nicol et al., 1987; Schnetkamp, 1987). The cGMP-induced fluxes observed in this study showed little evidence for two components with different kinetics (e.g., Fig. 5). In the experiment illustrated in Fig. 10, I have used the pharmacology of the cGMP-dependent channel to test whether cGMP-induced  $\text{Na}^+$  fluxes have two distinct components. One component of cGMP-induced  $\text{Ca}^{2+}$  release is fully activated by  $50 \mu\text{M}$  cGMP and can be blocked by tetracaine, but not by L-*cis* diltiazem; the other component of cGMP-induced  $\text{Ca}^{2+}$  release requires a much higher concentration of  $500 \mu\text{M}$  cGMP to be fully activated and is blocked by both L-*cis*

diltiazem and (less effectively) tetracaine (Koch et al., 1987; Schnetkamp, 1987). Drugs such as tetracaine and diltiazem are positively charged amphiphiles and adsorb strongly to negatively charged phospholipid bilayer membranes (much like neutral red); for this reason tetracaine and diltiazem have a strong effect on the surface potential and in our assay their use is limited to concentrations not exceeding 20  $\mu\text{M}$ . I used *D-cis* diltiazem, the stereoisomer of *L-cis* diltiazem which does not block the cGMP-dependent channel, as a control to cancel out the effect of the drugs on the surface potential.

If cGMP-induced  $\text{Ca}^{2+}$  fluxes observed with arsenazo III (Koch and Kaupp, 1985; Schnetkamp, 1987) are carried by the same channel responsible for cGMP-induced  $\text{Na}^+$  fluxes observed in this study, the latter should show two components with the following characteristics: cGMP-induced  $\text{Na}^+$  fluxes at 50  $\mu\text{M}$  cGMP should be blocked by tetracaine, but not by *L-cis* diltiazem, whereas cGMP-induced  $\text{Na}^+$  fluxes at 500  $\mu\text{M}$  cGMP should be blocked by both *L-cis* diltiazem and (less effectively) by tetracaine. The experiment illustrated in Fig. 10 shows exactly this pattern (similar results were obtained in eight other preparations for cGMP-induced  $\text{Ca}^{2+}$  and  $\text{Mg}^{2+}$  fluxes as well as for cGMP-induced fluxes of the other alkali cations tested). Note that in the presence of *L-cis* diltiazem the cGMP-induced  $\text{Na}^+$  fluxes at 50 and 500  $\mu\text{M}$  cGMP, respectively, were nearly identical as observed before for cGMP-induced  $\text{Ca}^{2+}$  fluxes measured with arsenazo III (Schnetkamp, 1987).

## DISCUSSION

### *An Optical Probe to Measure Cation Fluxes in Cell Suspensions*

Membrane vesicles derived from intact bovine ROS offer a convenient preparation to study the properties of the cGMP-dependent channel from a mammalian source with the optical probe neutral red; a single measurement with neutral red averages  $\sim 4 \times 10^8$  channels originating from 30 different animals. Binding of neutral red to the internal and the external surfaces of ROS membrane vesicles is sensitive to changes in intravesicular and external cation concentration, respectively; the properties of cation-induced changes in binding of neutral red are consistent with the notion that cations influence binding of neutral red via their effect on the surface potential at the membrane/water interface (Schnetkamp, 1985a; Figs. 1 and 2). The electrogenic protonophore FCCP in combination with a large proton buffer capacity of ROS membrane vesicles appeared to provide a current loop for inward cation currents through the cGMP-dependent channel; inward cation fluxes via the cGMP-dependent channel or via the added channel ionophore gramicidin were mirrored by outward proton fluxes (measured with the pH-indicating dye phenol red), and this provided a quantitative calibration of changes in light absorption (caused by unbinding of neutral red) into cation flux or current (Fig. 2). The relationship between changes in light absorption due to unbinding of neutral red and proton/cation fluxes was linear; this reflects the fact that the binding of both neutral red and protons to the membrane surface depends in an identical way on the surface potential since both carry a single positive charge.

The cGMP-dependent channel appeared to be the dominant conductive mechanism of  $\text{Na}^+$  transport present in ROS membrane vesicles. The average cGMP-

induced  $\text{Na}^+$  flux (at 100 mM  $\text{Na}^+$ ) in ROS membrane vesicles derived from a single ROS amounted to  $5 \times 10^6 \text{ Na}^+/\text{outer segment per s}$ , equivalent to a current of 0.8 pA, whereas  $\text{Na}^+$  currents in the absence of cGMP ranged between 0 and 0.1 pA;  $\text{Na}^+$  transport in the absence of cGMP increased upon aging and probably reflected passive leakage through the membrane. cGMP-induced fluxes were calculated from the initial rates of changes in light absorption, converted to fluxes with the help of the calibration plot illustrated in Fig. 2. A cGMP-induced current of 0.8 pA or an  $\text{Na}^+$  flux of  $5 \times 10^6 \text{ Na}^+/\text{ROS per s}$  can be compared with cGMP-induced  $\text{Ca}^{2+}$  release of  $1.1 \times 10^5 \text{ Ca}^{2+}/\text{ROS per s}$  from the same preparation of bovine ROS membrane vesicles measured with arsenazo III (Schnetkamp, 1987) or with cGMP-induced  $\text{Na}^+$  currents of 2 nA in excised patches of bovine ROS plasma membrane (Quandt et al., 1988 and manuscript submitted); those patches were derived from the same preparation of intact ROS that was used to prepare the ROS membrane vesicles in this study. The discrepancy in the magnitude of cGMP-induced currents observed in ROS membrane vesicles and excised patches of plasma membrane, respectively, suggests that the cGMP-dependent channels observed in ROS membrane vesicles reside in membranes with a much lower channel density than the plasma membrane. Only 20–25% of the bovine ROS vesicles contained functional cGMP-dependent channels (Figs. 3 and 4), similar to the fraction observed for cGMP-induced  $\text{Ca}^{2+}$  fluxes in bovine ROS membrane vesicles (Koch and Kaupp, 1985; Schnetkamp, 1987) or in leaky but otherwise undisturbed frog ROS (Schnetkamp and Bownds, 1987).

#### *Ion Selectivity of cGMP-dependent Channel in Bovine Rods*

The cGMP-dependent channel in bovine ROS membranes passed all alkali cations tested with a flux ratio of  $\text{Li} : \text{Na} : \text{K} : \text{Cs} = 0.8 : 0.8 : 1 : 0.6$ , and it passed all divalent cations tested with a flux ratio of  $\text{Mg} : \text{Mn} : \text{Ca} : \text{Sr} : \text{Ba} = 0.5 : 0.86 : 1 : 0.64 : 0.47$ , whereas no fluxes were observed for choline, and cGMP-induced  $\text{Ca}^{2+}$  fluxes (at 20 mM) were on average sevenfold smaller compared with cGMP-induced  $\text{Na}^+$  fluxes (at 100 mM). Qualitatively this is consistent with the observation that the apparent dissociation constant of the cGMP-dependent channel for  $\text{Ca}^{2+}$  is considerably smaller than for alkali cations. The above results are in general agreement with the ion selectivity of the light-sensitive current as measured in amphibian rods by means of rapid ion substitution experiments (Yau and Nakatani, 1984; Hodgkin et al., 1985; Cervetto et al., 1988; Menini et al., 1988), although the precise sequence and flux ratios differ somewhat between the different studies; these differences may arise from the different species or experimental protocols used (e.g., measuring inward currents versus measuring fluxes in the reverse direction). The properties of the cGMP-dependent channel purified and reconstituted from bovine ROS (Hanke et al., 1988) differ from the light-sensitive current in intact amphibian rod cells or from the results of this study with respect to their much lower efficacy in carrying  $\text{Li}^+$  and  $\text{Ca}^{2+}$  currents. Some of the apparent discrepancy may be resolved by the suggestion that two forms of the cGMP-dependent channel exist differing most noticeably in the ability to pass  $\text{Ca}^{2+}$  current (Cervetto et al., 1988).

The expert technical assistance of Mr. Robert T. Szerencsei was greatly appreciated. The author thanks Dr. R. J. French and D. L. J. Aha for critically reading earlier drafts of the manuscript.



This research was financially supported by grants from the Alberta Heritage Foundation for Medical Research and by the Medical Research Council of Canada.

*Original version received 1 August 1989 and accepted version received 30 March 1990.*

## REFERENCES

- Bauer, P. J. 1988. Evidence for two functionally different membrane fractions in bovine retinal rod outer segments. *Journal of Physiology*. 401:309–327.
- Caretta, A. 1985. Effect of cGMP and cations on the permeability of cattle retinal disks. *European Journal of Biochemistry*. 148:599–606.
- Caretta, A., and A. Cavaggioni. 1983. Fast ionic flux activated by cyclic GMP in the membrane cattle rod outer segments. *European Journal of Biochemistry*. 132:1–8.
- Caretta, A., A. Cavaggioni, and R. T. Sorbi. 1979. Cyclic GMP and the permeability of the disks of the frog photoreceptors. *Journal of Physiology*. 295:171–178.
- Cervetto, L., A. Menini, G. Rispoli, and V. Torre. 1988. The modulation of the ionic selectivity of the light-sensitive current in isolated rods of the tiger salamander. *Journal of Physiology*. 406:181–198.
- Cook, N. J., W. Hanke, and U. B. Kaupp. 1987. Identification, purification, and functional reconstitution of the cyclic GMP-dependent channel from rod photoreceptors. *Proceedings of the National Academy of Sciences USA*. 84:585–589.
- Fesenko, E. E., S. S. Kolesnikov, and A. L. Lynbasky. 1985. Induction by cyclic GMP of cationic conductance in plasma membrane of retinal rod outer segment. *Nature*. 313:310–313.
- Hanke, W., N. J. Cook, and U. B. Kaupp. 1988. cGMP-dependent channel protein from photoreceptor membranes: single-channel activity of the purified and reconstituted protein. *Proceedings of the National Academy of Science USA*. 85:94–98.
- Hodgkin, A. L., P. A. McNaughton, and B. J. Nunn. 1985. The ionic selectivity and calcium dependence of the light-sensitive pathway in toad rods. *Journal of Physiology*. 358:447–468.
- Koch, K. W., N. J. Cook, and U. B. Kaupp. 1987. The cGMP channel of vertebrate rod photoreceptors exists in two forms of different cGMP sensitivity and pharmacological behaviour. *Journal of Biological Chemistry*. 262:14415–14421.
- Koch, K. W., and U. B. Kaupp. 1985. Cyclic GMP directly regulates a cation conductance in membranes of bovine rods by a cooperative mechanism. *Journal of Biological Chemistry*. 260:6788–6800.
- Matthews, G. 1987. Single-channel recordings demonstrate that cGMP opens the light-sensitive channel of the rod photoreceptor. *Proceedings of the National Academy of Science USA*. 84:299–302.
- McLaughlin, A., C. Grathwohl, and S. McLaughlin. 1978. The adsorption of divalent cations to phosphatidylcholine bilayer membranes. *Biochimica Biophysica Acta*. 513:338–357.
- McLaughlin, S., N. Mulrine, T. Gresalfi, G. Vaio, and A. McLaughlin. 1981. Adsorption of divalent cations to bilayer membranes containing phosphatidylserine. *Journal of General Physiology*. 77:445–473.
- Menini, A., G. Rispoli, and V. Torre. 1988. The ionic selectivity of the light-sensitive current in isolated rods of the tiger salamander. *Journal of Physiology*. 402:279–300.
- Molday, R. S., D. Hicks, and L. L. Molday. 1987. Peripherin: a rim-specific membrane protein of rod outer segment discs. *Investigative Ophthalmology and Visual Sciences*. 28:50–61.
- Nicol, G. D., P. P. M. Schnetkamp, Y. Siami, E. Cragoe, and M. D. Bownds. 1987. A derivative of amiloride blocks both the light-regulated and cyclic GMP-regulated conductances in rod photoreceptors. *Journal of General Physiology*. 90:651–669.

- Quandt, F. N., G. D. Nicol, and P. P. M. Schnetkamp. 1988. Voltage dependency of gating of cyclic GMP-activated ion channels in bovine rod outer segments and block by 1-cis diltiazem. *Biophysical Journal*. 53:390a. (Abstr.)
- Schnetkamp, P. P. M. 1985a.  $\text{Ca}^{2+}$ -buffer sites in intact bovine rod outer segments: introduction to a novel optical probe to measure ionic permeabilities in suspensions of small particles. *Journal of Membrane Biology*. 88:249–262.
- Schnetkamp, P. P. M. 1985b. Ionic permeabilities of the plasma membrane of isolated intact bovine rod outer segments as studied with a novel optical probe. *Journal of Membrane Biology*. 88:263–275.
- Schnetkamp, P. P. M. 1986. Sodium-calcium exchange in the outer segments of bovine rod photoreceptors. *Journal of Physiology*. 373:25–45.
- Schnetkamp, P. P. M. 1987. Sodium ions selectively eliminate the fast component of guanosine cyclic 3', 5'-phosphate induced  $\text{Ca}^{2+}$  release from bovine rod outer segment disks. *Biochemistry*. 26:3249–3253.
- Schnetkamp, P. P. M., and M. D. Bownds. 1987.  $\text{Na}^{+}$ - and cGMP-induced  $\text{Ca}^{2+}$  fluxes in frog rod photoreceptors. *Journal of General Physiology*. 90:651–669.
- Schnetkamp, P. P. M., and U. B. Kaupp. 1985. Ca-H exchange in isolated bovine rod outer segments. *Biochemistry*. 24:723–727.
- Schnetkamp, P. P. M., U. B. Kaupp, and W. Junge. 1981. Interfacial potentials at the disk membranes of isolated intact cattle rod outer segments as a function of the occupation state of the intradiskal cation-exchange binding sites. *Biochimica Biophysica Acta*. 642:213–230.
- Schnetkamp, P. P. M., and R. T. Szerencsei. 1989. Silver ions induce a rapid  $\text{Ca}^{2+}$  release from isolated intact bovine rod outer segments by a cooperative mechanism. *Journal of Membrane Biology*. 108:91–102.
- Yau, K.-W., L. W. Haynes, and K. Nakatani. 1986. Roles of calcium and cGMP in visual transduction. In *Membrane Control of Cellular Activity*. H. Ch. Luttgau, editor. Gustav Fisher Verlag GmbH & Co. KG, Stuttgart. 343–366.
- Yau, K.-W., and K. Nakatani. 1984. Cation selectivity of light-sensitive conductance in retinal rods. *Nature*. 311:661–663.
- Yau, K.-W., and K. Nakatani. (1985). Light-suppressible, cyclic GMP-sensitive conductance in the plasma membrane of a truncated rod outer segment. *Nature*. 317:252–255.
- Zimmerman, A. L., G. Yamanaka, F. Eckstein, D. A. Baylor, and L. Stryer. 1985. Interaction of hydrolysis-resistance analogs of cyclic GMP with the phosphodiesterase and light-sensitive channel of retinal rod outer segments. *Proceedings of the National Academy of Sciences USA*. 82:8813–8817.